Control of the visibility profile in spectral low-coherence interferometry

Michael Hughes, Daniel Woods, and Adrian Gh. Podoleanu

We demonstrate that by obstructing half of one of the two beams from a low coherence interferometer before it is incident on the diffraction grating in a spectral interferometry set-up, we can generate an asymmetric profile for the visibility of the channeled spectrum (V) with optical path difference (OPD). Together with a lateral shift of the beam, as inspired by Talbot bands studies, this can be used to optimize V(OPD). We improve the model for the visibility of Talbot bands by considering the spectrometer resolution and demonstrate an improved Talbot band experiment. We also show that is possible to obtain regions of no interference around zero OPD.

Introduction

Spectral domain low coherence interferometry (SD-LCI) and Fourier domain optical coherence tomography (FD-OCT) employ a spectrometer at the output of a Michelson interferometer illuminated by a low coherence source. SD-LCI and FD-OCT suffer from a decay of sensitivity with OPD, V(OPD) [1] and mirror terms (i.e. the same modulation of the spectrum occurs for positive and negative OPD values) [2].

Wavetrain Model

In previous reports [3, 4] we have shown that the sensitivity decay, V(OPD) can be explained by considering the amount of overlap, C_{OR}, of the object and reference beam wavetrains after diffraction, overlap which also explains the Talbot bands phenomenon. In [4], we have shown that C_{OR} is given by the correlation of two functions, B_O and B_R (denoted B_1 and B_2 in [4]), which describe the field strength spatial profile at the grating within the object and reference beams respectively. In this report, we extend the theory to include effects due to the finite size of the CCD camera pixels by multiplying C_{OR} with the sinc term from theoretical models in [1] and [5], which yields a more complete expression:

$$V(OPD) = C_{OR}\left(\frac{\sin(\xi)}{\xi}\right)^2 \qquad (1)$$

where $\xi = (\pi / 2).(OPD / z_{RD})$ is the depth normalised by the first sinc zero, $Z_{RD} = \lambda^2 / (4\Delta\lambda)$, λ is the central wavelength, and $\Delta\lambda$ is the mean wavelength range which satisfies the grating equation for individual pixels (notation taken from [5]).

In conventional SD-LCI, B_O and B_R are described by Gaussians and the resultant correlation, C_{OR}, provides a Gaussian component of the visibility fall-off centred on OPD = 0, as predicted by consideration of the resolving power of the spectrometer in [1] and [5]. However, the models in [3] and [4] are more general providing for cases where the diffraction grating is illumined by non-super-imposed or non-Gaussian beams, allowing the profile of V(OPD) to be non-Gaussian or have a peak at OPD values away from zero.

Initial experimental studies [6] have demonstrated the effect of a lateral displacement of B_O from B_R for the limited case of beam separation equal to beam diameter – equivalent to the 'classic' Talbot experiment. However, the decay due to the sinc term was not quantified and the potential for profile shaping not explored.

In this letter we are now able to provide a more thorough model for the visibility decay and validate this model by actuating on the shape of the reference profile, B_R. Specifically, we employ this method for mirror term rejection.

Method

The experimental configuration used to demonstrate these effects (as shown in Fig. 1) is a LCI set-up capable of generating Talbot bands [4], improved from that presented in [6], so that no light is returned to the source. The interferometer is illuminated using an SLD power of 10 mW (central wavelength 840 nm, bandwidth 50 nm) and the spectrometer consists of a diffraction grating with 1200 lines/mm and a 2048 pixel linear CCD array (Aviiva M2 CL). Beam separation is adjusted by translating the fibre coupler in the object arm perpendicular to the optical axis and the OPD is adjusted by translating the same coupler axially. The size of the B_O and B_R is determined by microscope objectives MO_O and MO_R respectively. A second (2D) CCD camera (Cohu 6400 Series) monitors the relative positions and spatial profiles of the two spots on the grating. Profiles of V(OPD) were measured by placing a mirror at focus in the object and varying the OPD.

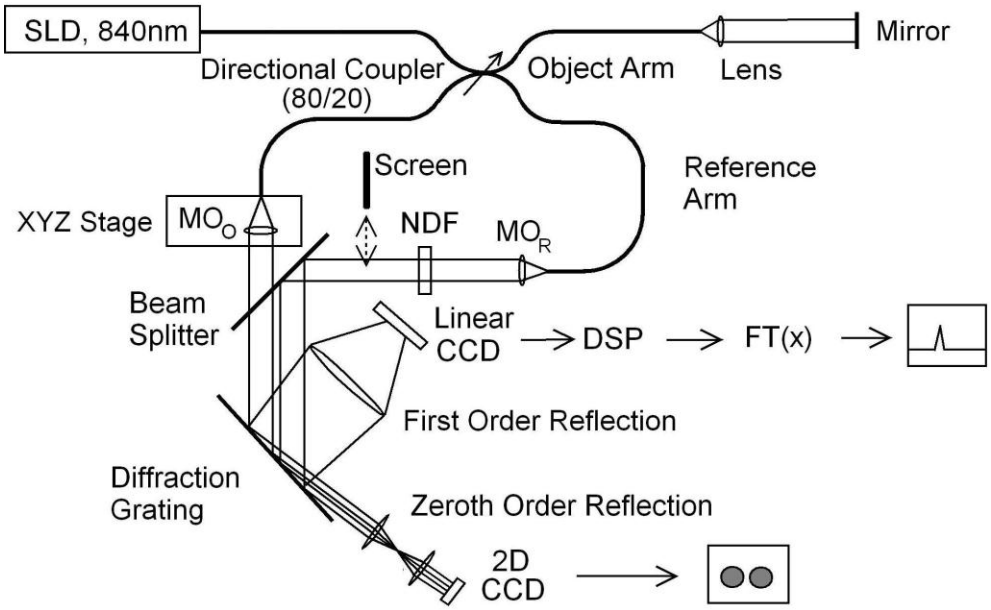

***Fig. 1**: Experimental LCI. NDF: Neutral Density Filter, MOR: Reference Beam Microscope Objective, MOO: Object Beam Microscope Objective, FT(x): 1D Fourier transform.*

Results

Fig. 2 shows profiles for various beam separations when the FWHM of both B_o and B_r is 1800 grating lines (MO_O and MO_R both x10 objectives). The theoretical profiles were generated using equation (1) with Z_{RD} = 3.50 mm. As predicted by [4], the increased separation of the spots shifts the peak of the sensitivity profile away from zero OPD, but conserves its shape and width as predicted by [3] and [4], with the amplitude subject to the sinc factor in equation (1). These results show that it is possible to have no detectable channelled spectrum for OPDs of less than zero, (elimination of the mirror terms), or, a novel feature, OPD intervals at zero OPD with no channelled spectrum.

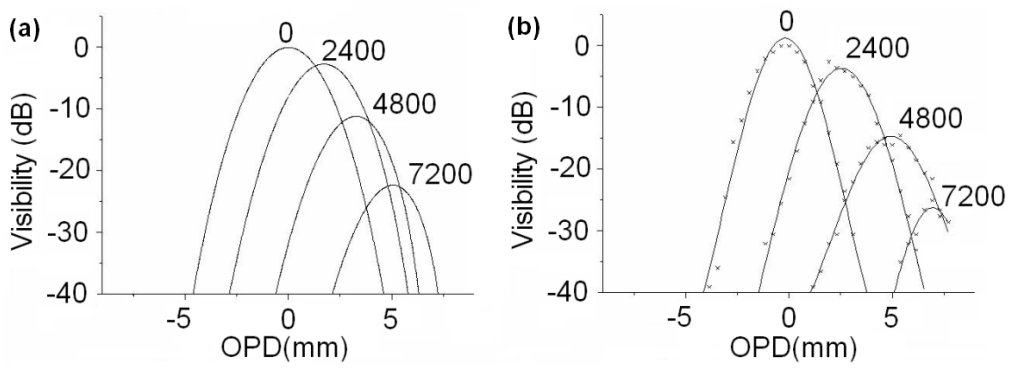

Fig. 2: *Sensitivity profiles (a) theoretical and (b) experimental for spot separations of 0, 2400, 4800 and 7200 grating lines.*

Our theory predicts that the spatial power distribution within the beams affects the distribution of power along the length of the diffracted wavetrains, which in principle allows for a comprehensive control of the visibility profile [4]. One application is the removal of mirror terms by manipulating the profile so as to have a step function at zero OPD. Unfortunately, this currently requires attenuation of the object arm which is clearly undesirable in most applications. We can, however, demonstrate the principle by using a smaller object beam spot size on the diffraction grating since, according to [4], as the object beam profile, B_O, tends towards a delta function, the sensitivity profile tends towards a (suitably scaled) copy of the reference beam profile, B_R.

Fig. 3 demonstrates an application of the method in producing an arrangement for rejecting mirror terms. The profile of B_R (MO_R = x10 objective, ~ 3600 diffraction grating lines) was initially shaped by placing a screen so as to block half of the beam. As can be seen in Fig. 3(a), the object beam diameter was reduced (using a x60 objective as MO_O) so as to have a FWHM of ~600 grating lines and the object beam was displaced by approximately 1000 grating lines to generate the shifting effect demonstrated in Fig. 2. The result, shown in Fig. 3(b) is, as predicted, an asymmetric profile (different from the symmetric profiles in Fig. 2) with a very sharp fall-off near zero OPD and an almost complete rejection of mirror terms (better than 45 dB at zero OPD). This new profile is compared with the conventional profile for a x10 object (MO_O) and a x60 reference (MO_R). The application to imaging systems here is clear, since it is possible to work with the OPD = 0 position deep inside scattering objects without mirror terms occurring.

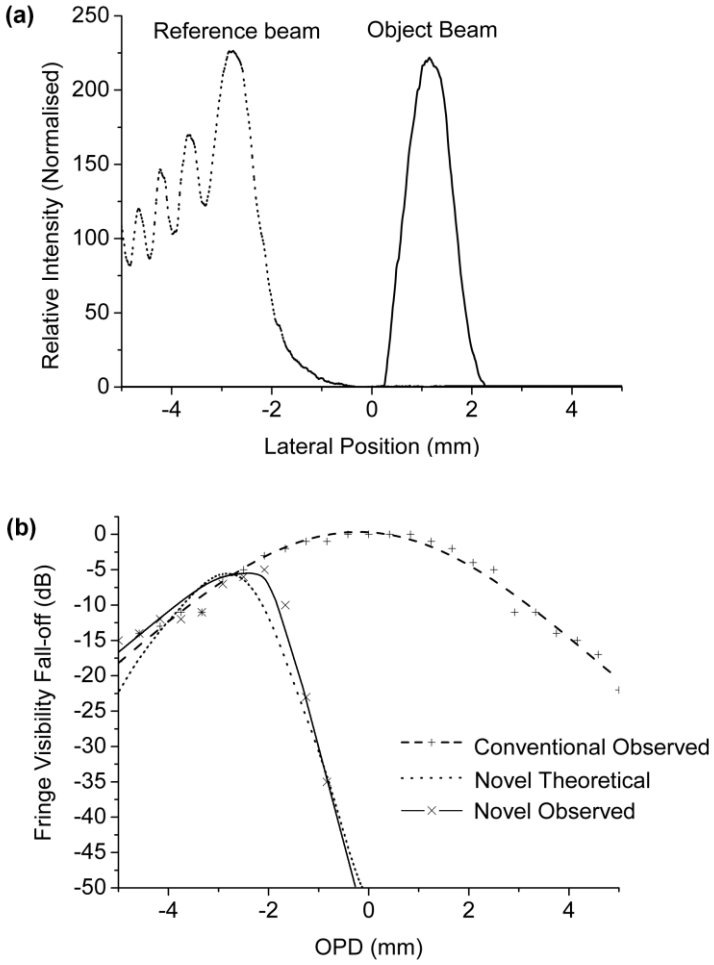

Fig. 3: *Configuration for mirror term rejection, showing (a) spatial profiles of object spot (600 lines, displaced 1000 lines) and reference spot (3500 lines, half blocked) and (b) resulting visibility profile showing sharper transition at OPD=0, compared to conventional profile (both beams superposed, no screen).*

Conclusion

We have provided the first general experimental verification that the visibility profile is dependent not only on the relative positions of the object and reference beams on the diffraction grating but on their spatial profiles as well., We have created a range of OPD values starting from zero where no channeled spectrum is generated, a technique which may find applications in the field of sensor multiplexing. In addition we have shaped the profile of the fall-off to produce a step function at zero OPD in conjunction with elimination of mirror terms, which may find applications in OCT in general, and in the OCT of moving tissue in particular, as the elimination of the opposite sign of OPD is not disturbed by movement. Previous reports [1, 5] based on only the spectrometer resolution cannot explain the effects seen here.

References

1. HU, Z., PAN, Y., and ROLLINS, A.M., "Analytical model of spectrometer-based two-beam spectral interferometry," Appl. Opt. 46, pp. 8499-8505 (2007).

2. ZHANG, J. et al., "Removal of a mirror image and enhancement of the signal-to-noise ratio in Fourier-domain optical coherence tomography using an electro-optics phase modulator," Opt. Lett. 30, pp. 147-149 (2005).

3. PODOLEANU, A., "Unique interpretation of Talbot bands and Fourier domain white light interferometry," Opt. Express 15, pp. 9867-9876 (2007).

4. WOODS, D., PODOLEANU, A., "Controlling the Shape of Talbot Bands Visibility," Opt. Express 16, pp. 9654-9670 (2008).

5. YUN, S.H. et al., "High-speed spectral-domain optical coherence tomography at 1.3um wavelength," Opt. Express 11, pp. 3598–3604 (2003).

6. PODOLEANU, A., and WOODS, D., "Power-efficient Fourier domain optical coherence tomography setup for selection in the optical path difference sign using Talbot bands," Opt. Lett. 32, pp. 2300-2302 (2007).

Authors' affiliations:

Michael Hughes, Daniel Woods, and Adrian Podoleanu: Applied Optics Group, School of Physical Sciences, University of Kent, Canterbury, CT1 7NH, England.
michael.robert.hughes@gmail.com